JOURNAL OF VIROLOGY, June 2006, p. 6033–6047 Vol. 80, No. 12
0022-538X/06/$08.00+0 doi:10.1128/JVI.02108-05

Cellular and Biochemical Differences between Two Attenuated Poxvirus Vaccine Candidates (MVA and NYVAC) and Role of the C7L Gene

José Luis Nájera, Carmen Elena Gómez, Elena Domingo-Gil, María Magdalena Gherardi,† and Mariano Esteban*

Department of Molecular and Cellular Biology, Centro Nacional de Biotecnología, CSIC, Ciudad Universitaria Cantoblanco, 28049, Madrid, Spain

Received 6 November 2005/Accepted 13 February 2006

The poxvirus strains NYVAC and MVA are two candidate vectors for the development of vaccines against a broad spectrum of diseases. Although these attenuated virus strains have proven to be safe in animals and humans, little is known about their comparative behavior in vitro. In contrast with MVA, NYVAC infection triggers greater cytopathic effect in a range of permissive and nonpermissive cell lines. The yields of NYVAC cell-associated virus in permissive cells (BHK-21) were slightly reduced compared with those of MVA infection. During the course of infection in HeLa cells, there is a translational block induced by NYVAC late in infection, which correlated with a marked increase in phosphorylation levels of the initiation factor eIF-2α. In contrast to MVA, the synthesis of certain late viral proteins was only blocked in NYVAC-infected HeLa cells. Electron microscopy (EM) analysis revealed that morphogenesis of NYVAC in HeLa cells was blocked at the stage of formation of immature viral forms. Phase-contrast microscopy, EM, flow cytometry, and rRNA analyses demonstrated that contrary to MVA, NYVAC infection induces potent apoptosis, a phenomenon dependent on activation of caspases and RNase L. Apoptosis induced by NYVAC was prevented when the virus gene C7L was placed back into the NYVAC genome, recovering the ability of NYVAC to replicate in HeLa cells and maintaining the attenuated phenotype in mice. Overall, our findings demonstrate distinct behavior between NYVAC and MVA strains in cultured cells, as well as a new role for the C7L viral gene as an inhibitor of apoptosis in NYVAC infection.

Poxvirus vectors are considered to be prime candidates for use as recombinant vaccines due to their efficient expression of the foreign antigen and unique immunological properties in eliciting long-term protective humoral and cell-mediated immune responses (44). Increased immunosuppression as a result of human immunodeficiency virus (HIV) infection, cancer treatments, and organ transplantation, in addition to the possible vaccination of the general public due to the emerging threat of smallpox bioterrorism, requires the need for the development of safe and efficacious vectors (46). Numerous approaches have been taken to enhance the safety of poxviruses. These include the replication-deficient modified vaccinia virus Ankara (MVA) (21), nonreplicating defective vaccinia virus (VV) (46), host cell-restricted vectors such as avipoxviruses (ALVAC) (72), fowlpox virus (44), and poxvirus vectors with deletions in nonessential genes (60), such as those coding for serpins (37), or host range genes, such as the NYVAC strain (71). In this regard, recombinants based on MVA or NYVAC strains are emerging as important candidates to be used as live vaccines against numerous infectious diseases and in cancer therapy.

The current widely used MVA strain was classically attenuated by growing the virus after more than 500 passages in chicken embryo fibroblasts (CEF) (40). During the course of attenuation, 15% of the parental viral genome was lost (1) as was the ability to grow in human cells and a majority of mammalian cells (15, 20, 43). MVA has been shown to be safe in humans, with no adverse side effects, as demonstrated when over 120,000 individuals were vaccinated during the smallpox eradication campaign (40). At present, first-generation recombinant MVA vaccines inducing relevant recombinant antigen-specific T-cell immunogenicity in humans have been clinically tested against infectious disorders such as AIDS, malaria, and human papillomavirus-associated cancer (for review, see reference 68).

The NYVAC vector was derived from the Copenhagen strain of VV. It was genetically attenuated by the deletion of 18 nonessential genes implicated in virulence, host range, or pathogenicity, resulting in a strain with a highly debilitated in vitro replicative capacity on cells derived from humans, mice, and equid origin, but with the ability to replicate with wild-type efficiency in CEFs and Vero cells (69–71). A number of examples employing the NYVAC vector as a recombinant vaccine delivery system have been provided in various animal models and humans with promising results (50, 52, 69). Although NYVAC is a highly attenuated virus, it retained the ability to induce a protective immune response to foreign antigens in a similar way to the thymidine kinase mutant of the parental strain (49). To date, all of the data obtained from human clinical trials using NYVAC-based vectors illustrate a positive safety profile and the induction of high levels of immunity against the expressed heterologous antigens (10, 12, 19, 23, 32, 47, 50, 53).

* Corresponding author. Mailing address: Department of Molecular and Cellular Biology, Centro Nacional de Biotecnología, CSIC, Ciudad Universitaria Cantoblanco, 28049, Madrid, Spain. Phone: 34-91-585-4553. Fax: 34-91-585-4506. E-mail: mesteban@cnb.uam.es.

† Present address: National Reference Center for AIDS, Department of Microbiology, School of Medicine, University of Buenos Aires, Buenos Aires, Argentina.

Even though the attenuated poxvirus vectors MVA and NYVAC have been widely characterized in terms of safety and immunogenicity, a careful evaluation of the differences in MVA and NYVAC biology remains to be established. A comparative analysis of expression profiles obtained by cDNA microarray screening of over 15,000 human genes in NYVAC- or MVA-infected HeLa cells revealed that both virus strains induced common and distinct proinflammatory cytokine profiles (30, 31).

In this study, we examined the in vitro behavior of NYVAC in comparison with that of MVA using cellular and biochemical approaches. Our findings revealed distinct biological characteristics of MVA and NYVAC strains, which are likely to influence the immunogenicity of these recombinant vectors when used as vaccines. Among the candidate genes deleted in NYVAC and intact in the MVA genome (1), we found the C7L gene responsible for the distinct biological differences between both attenuated strains.

MATERIALS AND METHODS

Cells and viruses. Cells were maintained in a humidified air–5% CO_2 atmosphere at 37°C. African green monkey kidney cells (BSC-40) and human cells (HeLa) were grown in Dulbecco's modified Eagle's medium (DMEM) supplemented with 10% newborn calf serum. Mouse 3T3-like fibroblast cells (3T3), baby hamster kidney cells (BHK-21), CEF, and human cells (TK-143) were grown in DMEM supplemented with 10% fetal calf serum (FCS). The VV strains used in this work include Western Reserve (WR), MVA obtained after 586 passages in CEFs (passage 585 of MVA was kindly provided by G. Sutter, Munich, Germany), and NYVAC (provided by J. Tartaglia from Aventis-Pasteur). These strains were grown and titrated in BSC-40 cells (WR) or in CEFs (MVA or NYVAC). All viruses were purified by two sucrose cushions and titrated by immunostaining (25). The particle/PFU ratio in the different virus preparations was determined by measurements of optical density at 260 nm (OD_{260}) and virus titration (1 OD_{260} unit represents 1.2×10^{10} particles per ml) (22).

Generation of NYVAC-C7L. The C7L gene was obtained by PCR of genomic MVA DNA using the following set of primers: 5′-CGGGATCCCATGGGTAT ACAGCACGAATTCG (BamHI site underlined) and 5′-TCCCCCGGGTAAT CCATGGACTCATAATCTCTATACG (SmaI site underlined). The amplified DNA fragments were digested with restriction endonucleases BamHI and SmaI and cloned into pJR101 vector (27) previously digested with BglII and SmaI. The resulting plasmid, pJR101-C7L, directs the insertion of the C7L gene into the hemagglutinin locus of the NYVAC genome under the transcriptional control of the synthetic early/late (E/L) promoter. BSC-40 cells were infected with the attenuated NYVAC strain at a multiplicity of 0.01 PFU/cell and then transfected with 10 μg of DNA from plasmid pJR101-C7L using Lipofectamine reagent according to the manufacturer's instructions (Invitrogen). Recombinant NYVAC viruses containing the C7L gene were selected by consecutive rounds of plaque purification in BSC-40 cells stained with X-Gluc (5-bromo-4-chloro-3-indoxyl-β-D-glucuronidase acid). Purity of the recombinant NYVAC-C7L virus was confirmed by PCR and by DNA sequence analysis.

Evaluation of CPE by phase-contrast microscopy. In the evaluation of cytopathic effects (CPE) under permissive and nonpermissive conditions, the indicated cell lines were seeded into 12-well tissue culture plates and grown to confluence. The cells (duplicate wells) were infected at 5 PFU/cell with WR, MVA, NYVAC, or NYVAC-C7L and visualized under a phase-contrast microscope at various times postinfection (p.i.) for CPE (such as cell rounding, cytoplasmic contraction, and slow detachment). In addition, we analyzed this effect in infected HeLa cells treated with a DNA synthesis inhibitor, Ara C, at a concentration of 50 μg/ml. A total of three independent experiments were performed.

Analysis of virus growth. To determine virus growth profiles, monolayers of HeLa or BHK-21 cells grown in 12-well tissue culture plates were infected at 0.01 PFU/cell with WR, MVA, or NYVAC strains. Following virus adsorption for 60 min at 37°C, the inoculum was removed. The infected cells were washed twice with DMEM without serum and incubated with fresh DMEM containing 2% of FCS at 37°C in a 5% CO_2 atmosphere. At different times postinfection, cell supernatants were removed by scraping with a pipette and cells in the monolayer were independently collected in serum-free medium. The supernatants were stored at 4°C for no more than 48 h before virus titration, and cell-associated virus in the collected monolayer was released from cells by freeze-thawing and brief sonication. Serial dilutions of the resulting cell lysates and of supernatants were plated on confluent BHK-21 monolayers grown in six-well plates in duplicate. Following virus adsorption for 60 min at 37°C, the inoculum was removed. The infected cells were washed twice with DMEM without serum and incubated with fresh DMEM containing 2% of FCS at 37°C in a 5% CO_2 atmosphere. Following 24 h postinfection, the virus titers were determined by immunostaining assay with anti-VV antibodies as previously described (33). At least three independent virus titrations were performed with the samples containing the virus released to the medium during infection (supernatant) and the virus that remained cell associated (monolayer cells).

Metabolic labeling of proteins. HeLa and BHK-21 cells grown in 12-well plates were infected at 5 PFU/cell with MVA or NYVAC. At different times postinfection (4, 8, and 16 h), cells were rinsed three times and incubated with Met-Cys-free DMEM 30 min prior to labeling. After incubation, the medium was removed and 50 μCi of [^{35}S]Met-Cys Promix per ml in Met-Cys-free DMEM was added for an additional 30 min. After three washes with phosphate-buffered saline (PBS), cells were resuspended in Laemmli sample buffer, and equal amounts of proteins (20 μg) were analyzed by sodium-dodecyl sulfate-polyacrylamide gel electrophoresis (SDS-PAGE) followed by autoradiography.

Western blot analysis. Antibodies that specifically recognize the products of viral early and late genes, such as E3L (p25), A14L (p16), A4L (p39), A17L (p21), A27L (p14), and L1R (p27.5), were used in the identification of viral proteins. Anti-E3L was kindly provided by B. Moss and B. Jacobs and anti-L1R by Y. Ichihashi. The remaining antibodies were generated in our laboratory and have been described previously (17, 57, 59, 61). The rabbit polyclonal antiserum raised against live VV was previously described (57). The rabbit polyclonal anti-eIF2α phospho-specific antibody was supplied by BIOSOURCE. The monoclonal antibody against β-actin was supplied by Sigma. Rabbit polyclonal anti-eIF2α antibody was supplied by Santa Cruz Biotechnology, Santa Cruz, CA. Rabbit polyclonal anti-human poly(ADP)-ribose polymerase (PARP) was supplied by Cell Signaling.

For Western blot analyses, total cell extracts were boiled in Laemmli sample buffer, and proteins were fractionated by 10% SDS-PAGE. Following electrophoresis, proteins were transferred to nitrocellulose membranes using a semidry blotting apparatus (Gelman Sciences). The filters were incubated for 30 min with PBS containing nonfat dry milk at 5% (BLOTTO) at room temperature, mixed with antisera in BLOTTO, incubated overnight at 4°C, washed three times with PBS, and further incubated with secondary antibodies coupled to horseradish peroxidase in BLOTTO. After the PBS wash, the immunocomplexes were detected by enhanced chemiluminescence (ECL) Western blotting reagents (Amersham).

RT-PCR. HeLa cells cultured in six-well plates were mock infected or infected with WR, MVA, NYVAC, or NYVAC-C7L at 5 PFU/cell. Total RNA was isolated at 24 h p.i. using the Ultraspec-II RNA resin purification system (Biotecx) following the manufacturer's instructions. Total RNA (1.5 μg) was digested with DNases to avoid genomic DNA contamination (Ambion Turbo kit). PCR with *Taq* Platinum DNA polymerase (Invitrogen) and primers for a control viral gene was performed to ensure there was no DNA contamination (data not shown). Reverse transcription-PCR (RT-PCR) was carried out with 150 ng of total RNA (free of DNA contaminant) using the Invitrogen ONE-STEP kit. Primers for amplification of E3L were 5′-GAGATTGTGTGTGAGGCT and 3′-AAAAGACCAATCTCTTCT. Primers for A27L were (forward) 5′GCGCT CGAGATGCATCATCATCATCATGACGGAACTCTTTTCCCC and (reverse) 5′-CGCGGTACCTTACTCATATGGGCGCCGTCCAGTC.

Primer extension. Primer extension was carried out under the following conditions: 2 pmol of VIC-labeled primer from Applied Biosystems (specific for the viral A27L gene), 2 μg of total RNA, and 0.5 mM of deoxynucleoside triphosphate (dNTP) mix in a 0.5-ml microcentrifuge tube. Samples were heated at 65°C for 5 min before quenching in ice for at least 5 min. First-strand cDNA synthesis was performed using SuperScript II RT and 5× RNX buffer (Invitrogen) according to the manufacturer's instructions for 50 min at 42°C. Samples were next incubated for 15 min at 70°C and quenched in ice before precipitation. VIC-labeled cDNAs were allowed to precipitate for 30 min at 40°C following the addition of 0.7 volume of isopropanol. cDNAs were pelleted by centrifugation at 15,000 rpm for 10 min and washed with 70% ethanol before being air dried and stored at −20°C. Each cDNA sample was dissolved in a solution consisting of 2.5 μl formamide (Promega), 0.5 μl GeneScan −500 ROX internal lane standard (Applied Biosystems), and 2 μl of loading buffer (Applied Biosystems) per sample. The primer extension products were sized using the GeneScan analysis software version 3.7 (Applied Biosystems).

Electron microscopy. Monolayers of HeLa cells were infected at 5 PFU/cell with MVA or NYVAC. At 16 h p.i., cells were fixed in situ with a mixture of 2% glutaraldehyde and 1% tannic acid in 0.4 M HEPES buffer (pH 7.5) for 1 h at room temperature. Fixed monolayers were removed from culture dishes in a fixative and transferred to Eppendorf tubes. After centrifugation and a wash with HEPES buffer, the cells were stored at 4°C until used. For ultrastructural studies, fixed cells were processed for embedding in epoxy resin EML-812 (TAAB Laboratories, Ltd., Berkshire, United Kingdom) as previously described (57). Postfixation of cells was completed with a mixture of 1% osmium tetroxide and 0.8% potassium ferricyanide in distillate water for 1 h at 4°C. After two washes with HEPES buffer, samples were treated with 2% uranyl acetate, washed again, and dehydrated in increased concentrations of acetone for 10 min each time at 4°C. Infiltration in resin was done at room temperature for 1 day. Polymerization of infiltrated samples was done at 60°C for 3 days. Ultrathin sections (20 to 30 nm thick) of the samples were stained with saturated uranyl acetate and lead citrate by standard procedures. Collection of images from negative staining and ultrathin sections was done in a JEOL 1200-EX II electron microscope operating at 100 kV (25, 57).

DAPI staining. HeLa cells were grown to confluence in 12-well plates containing 12-mm-diameter glass coverlips were either uninfected or infected with WR, MVA, or NYVAC at 5 PFU/cell. Cells were stained at 24 h p.i. with 4′,6′-diamidino-2-phenylindole (DAPI; 10 μg/ml) for 30 min at room temperature and photographed under a fluorescence microscope.

rRNA breakdown. HeLa cells cultured in six-well plates were mock infected or infected with WR, MVA, NYVAC, or NYVAC-C7L at 5 PFU/cell. Total RNA was isolated at 18 and 24 h p.i. using the Ultraspec-II RNA resin purification system (Biotecx) following the manufacturer's instructions. Fractionation of rRNA was performed by electrophoresis in 1% agarose formaldehyde gel containing 2 μg of total RNA per lane. Breakdown of rRNA was visualized after staining the gel with ethidium bromide.

Measurement of apoptotic cell death by cell cycle analysis. The different stages of the cell cycle and the percentage of cells with sub-G_0 DNA content were analyzed by propidium iodide (PI) staining (38). Briefly, HeLa cells were infected at 5 PFU/cell with WR, MVA, NYVAC, or NYVAC-C7L in the presence or absence of the general caspase inhibitor zVAD-fmk (40 μM; Calbiochem). Mock-infected cells were used as a negative control. At 24 h p.i., cells were removed by pipetting, washed once with cold PBS, and permeabilized with 70% ethanol in PBS at 4°C overnight. After three washes with PBS, the cells were incubated for 45 min at 37°C with RNase A and stained with PI (10 μg/ml). The percentage of cells with hypodiploid DNA content was determined by flow cytometry. Data were acquired for 15,000 cells per sample and analyzed as described above, and the results are expressed as fold increase in apoptotic cells with respect to uninfected cells.

Virus pathogenicity. Groups of 10-week-old female BALB/c mice ($n = 4$ per group) were inoculated intranasally (i.n.) with different challenge doses of NYVAC or NYVAC-C7L (10^6 to 10^8 PFU/mouse) or with 10^6 PFU/mouse of WR (diluted in 50 μl of PBS). The mortality and body weight loss were monitored for at least 2 weeks, with daily measurements of individual animals. Animals suffering from severe systemic infection and having lost >25% body weight were sacrificed. The mean change in body weight was calculated as the percentage of the mean weight for each group on the day of challenge.

RESULTS

NYVAC infection triggered more severe CPE than MVA in permissive and nonpermissive cell lines. Infection with VV induces dramatic changes in cell functions, metabolism, and morphology, all of which are collectively termed the CPE (2, 4, 6). In order to characterize the CPE produced by the VV strains WR, NYVAC, and MVA, monolayers of different cell lines (permissive and nonpermissive) were infected at 5 PFU/cell with each virus and the extent of CPE was analyzed by phase-contrast microscopy at different times postinfection. The particle/PFU ratios determined in the different viral preparations were 302 for MVA, 272 for NYVAC, and 310 for WR, demonstrating the same infectivity of the purified viruses. Characteristics such as cytoplasmic contraction, cell rounding, and cell detachment were monitored. The cell lines infected with NYVAC (HeLa, BHK-21, BSC-40, and 3T3), independently of the host restriction, exhibited evident cell rounding as early as 2 h p.i. Representative findings are shown for HeLa cells (Fig. 1). During the course of NYVAC infection, the CPE increased with time, and by 24 h p.i, a high level of cell detachment was noted. The same effects were observed in NYVAC-infected cells treated with Ara C, a drug that blocks DNA replication (not shown). In contrast, the CPE was delayed and significantly reduced in cells infected with MVA (Fig. 1). The morphology of the CPE in NYVAC-infected cells, but not in WR or MVA infections, at late times was reminiscent of apoptosis.

Virus growth of MVA and NYVAC in permissive and nonpermissive cell lines. Deletion of two of the host range genes K1L and C7L in the NYVAC genome is associated with a reduced ability of the virus to replicate within a broad range of cell lines of human origin, as well as rabbit kidney and pig kidney cells (48, 71). Nonetheless, NYVAC can replicate with wild-type efficiency in Vero cells and primary CEF (69, 70). The host range phenotype observed with MVA includes a characteristic late block upon nonproductive infection of many mammalian cells, with unimpaired viral DNA replication and late gene expression (67, 76). As previously described, the restriction exhibited by MVA in nonpermissive cell lines is a consequence of a defect in virus morphogenesis (11, 17, 39). The restriction observed in NYVAC may also be due to a defect in virus morphogenesis or virus spread. To analyze the viral growth characteristics of MVA and NYVAC under permissive and nonpermissive conditions, monolayers of BHK-21 and HeLa cells were infected at 0.01 PFU/cell with each virus for 0, 24, 48, and 72 h. Infectious viruses that remained cell-associated and were released to the medium during the course of the infection were measured by an immunostaining assay. For comparative purposes, we used the replication-competent WR strain. In HeLa cells infected with WR, the virus titer increased with time more than 10,000-fold, while there was no increase in virus titer with either MVA nor NYVAC infection (Fig. 2A and B). In contrast, under permissive conditions, the growth kinetics of the three virus strains were similar (Fig. 2C and D). Interestingly, the titers of cell-associated virus in BHK-21 cells infected with NYVAC were lower than the titers obtained in cells infected with WR or MVA (Fig. 2C). This finding was consistent in three independent experiments. The results of Fig. 2 demonstrate that under nonpermissive conditions, there is a similarly restricted production of infectious viral particles in NYVAC- and MVA-infected cells, while under permissive conditions, the total viral yields are not affected. Nonetheless, the virus that remains cell associated late in infection is reduced in NYVAC-infected cells compared to that in MVA- or WR-infected cells. This reduction is probably the consequence of the severe cell destruction that followed NYVAC infection (see Fig. 1).

Protein synthesis during NYVAC and MVA infection. In order to compare the shutoff and kinetics of synthesis of viral proteins in permissive and nonpermissive cell lines infected with MVA and NYVAC, BHK-21 and HeLa cells were infected at 5 PFU/cell with each virus, and at 2, 4, 8, and 16 h p.i., the infected cells were metabolically labeled for 30 min with [^{35}S]Met-Cys Promix. Cell lysates were fractionated by SDS-PAGE, and the protein pattern examined by autoradiography. As shown in Fig. 3A, in BHK-21 cells infected with MVA and

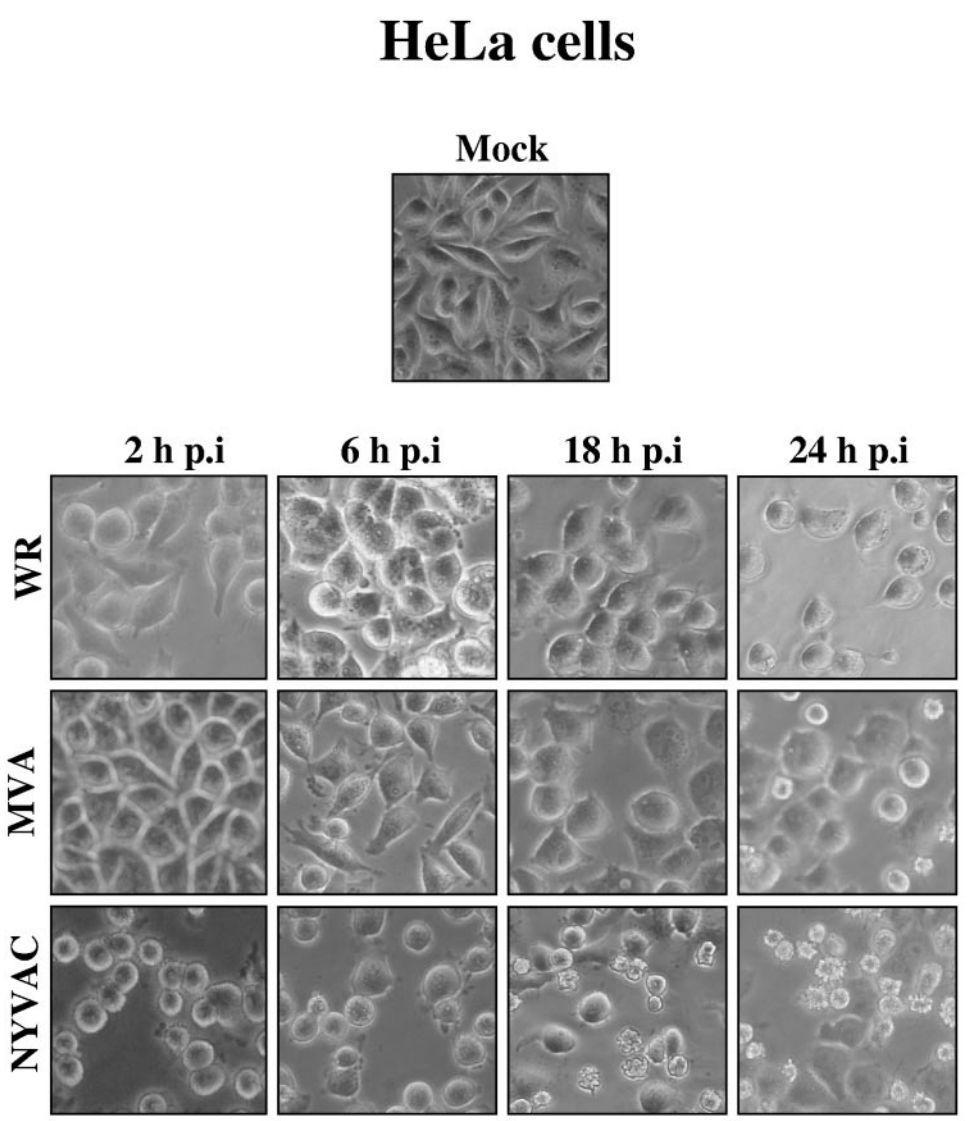

FIG. 1. CPE of MVA and NYVAC in human cells. Monolayers of HeLa cells were mock infected or infected at 5 PFU/cell with WR, MVA, or NYVAC. At different times postinfection, as indicated in the figure, the morphological changes in the cells were examined by phase-contrast microscopy. Mock, uninfected cells.

NYVAC, the pattern of viral proteins and the shutoff of cellular proteins occur with similar kinetics between the two viruses, although some differences were noted in protein abundance. This was confirmed by Western blot analysis from the same cell homogenates. Accumulation of viral proteins during infection was reduced in NYVAC-infected cells compared with MVA-infected BHK-21 cells (Fig. 3C). In HeLa cells infected with NYVAC or MVA, a similar pattern of viral proteins was observed between the two viruses, while the shutoff was more pronounced in cells infected with NYVAC late in infection (Fig. 3B). Some differences were also noted in protein abundance between NYVAC and MVA, a finding confirmed by Western blot analysis (Fig. 3D). The accumulation of viral proteins in NYVAC-infected permissive and nonpermissive cells was reduced compared with that in MVA-infected cells, which could be due to a defect in translation or transcription or a cell lysis effect. It is well established that phosphorylation of the α subunit of the eukaryotic translation initiation factor 2 (eIF-2) on serine 51 leads to the downregulation of translation initiation (62). As such, we determined whether NYVAC infection alters this initiation step. Thus, the levels of phospho-eIF-2α-S51 in BHK-21 and HeLa cells infected with MVA or NYVAC were determined by immunoblot analysis with specific anti-eIF-2α-S51 antibody. As shown in both cell lines (Fig. 3E and F), a low level of phosphorylated eIF2-α was detectable in mock-infected cells and at early times after NYVAC or MVA infection. However, with time of infection there was an increase in eIF2-α phosphorylation in cells infected with NYVAC but not in cells infected with MVA. The increase in eIF2-α phosphorylation correlates with the shutoff of host protein synthesis, suggesting that levels of viral proteins in NYVAC-infected cells could be compromised by the extent of eIF2-α phosphorylation induced by the virus.

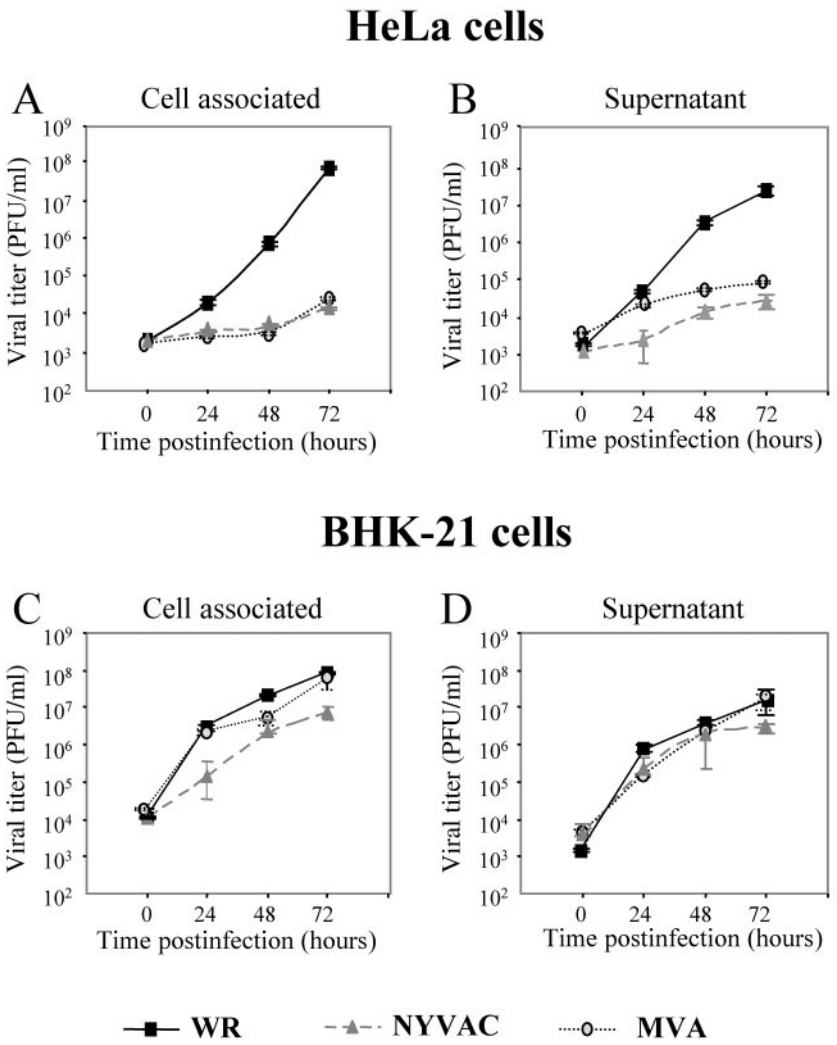

FIG. 2. Virus growth of MVA and NYVAC in permissive and nonpermissive cell lines. Monolayers of HeLa and BHK-21 cells were infected at 0.01 PFU/cell with WR, MVA, or NYVAC for 0, 24, 48, and 72 h. Cells were collected by centrifugation, and infectious virus associated with the cells (A and C) and released to the supernatant (B and D) during the course of the infection was quantified by immunostaining assay. For comparative purposes, we used the replication-competent WR strain. Averages of three independent experiments are shown with standard error bars.

Differences in late viral proteins between MVA and NYVAC infection in nonpermissive cells. Poxvirus gene expression is regulated in a cascade manner. As such, early genes are transcribed immediately following infection by enzymes and transcription factors contained within the infecting virion, while late and intermediate genes are transcribed after the start of viral DNA replication (13, 41, 45). Consequently, in view of the translational control exerted by phosphorylation of eIF-2α during NYVAC infection, we next determined if the translation of specific early and late viral genes was blocked. This was analyzed by Western blotting in cell lysates of BHK-21 and HeLa cells infected with WR, MVA, or NYVAC, using different antibodies that specifically recognized the early viral protein p25 (E3L) and the late viral proteins p14 (A27L), p21 (A17L), p16 (A14L), p39 (A4L), and p27.5 (L1R). As shown in Fig. 4A, under permissive conditions, early and late viral proteins were efficiently detected in lysates of cells infected with WR, MVA, or NYVAC. However, under nonpermissive conditions, apparent differences in specific proteins were observed between NYVAC and MVA. Early viral proteins were efficiently detected in lysates of cells infected with the three viruses. In contrast, late viral proteins that corresponded to the gene products of A27L, A17L, and L1R were not detected in the lysates of cells infected with NYVAC, while in lysates from cells infected with MVA or WR, all proteins were produced. Interestingly, other late proteins such as p16 (A14L) and p39 (A4L) were efficiently detected in NYVAC-infected cells. Similar results were confirmed by confocal immunofluorescence analysis (data not shown).

To determine a possible defect at the transcriptional level, we analyzed early and late transcription of viral genes in WR-, MVA-, and NYVAC-infected HeLa cells. For this purpose, total RNA was isolated at 24 h p.i. and mRNA levels of a specific viral early gene (E3L) and a late viral gene (A27L)

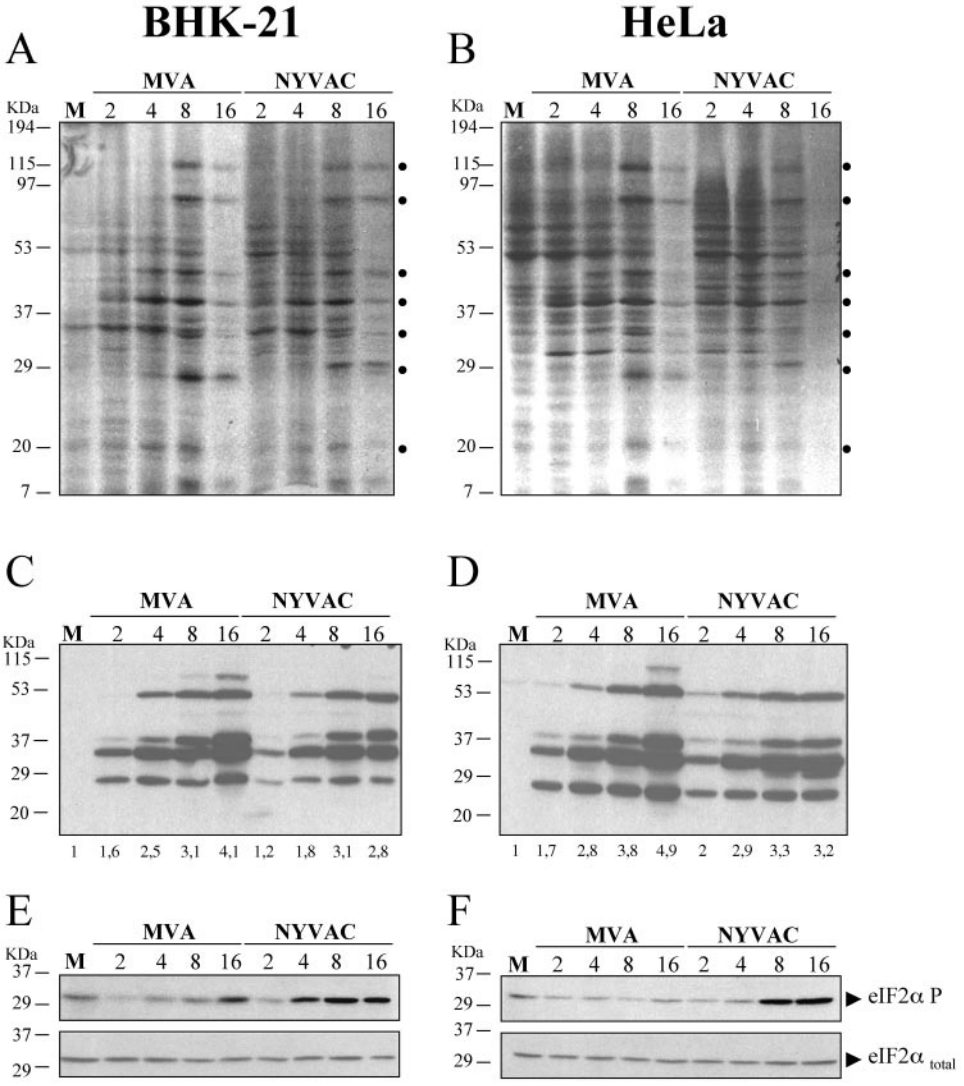

FIG. 3. Protein synthesis during NYVAC and MVA infection. Monolayers of BHK-21 (A) and HeLa (B) cells were mock infected (M) or infected at 5 PFU/cell with MVA or NYVAC. At the indicated times (h p.i.), cells were metabolically labeled for 30 min with [^{35}S]Met-Cys Promix (50 μCi/ml) and equal amounts of proteins were analyzed by SDS-PAGE (10%) and autoradiography. The dots on the right indicate prominent viral proteins. (C and D) Western blot showing expression of VV antigens during the time course of MVA and NYVAC infection in infected BHK-21 (C) and HeLa (D) cells. The blot was probed with a rabbit polyclonal antiserum (1:500 dilution) raised against live VV. Numbers appearing under each lane represent the ratio of intensity of the bands in infected cells to levels in uninfected cells, as determined by densitometric analyses. (E and F) Western blot analysis of total eIF2-α and phospho-eIF-2α-S51 protein levels during the time course of MVA and NYVAC infection in infected BHK-21 (E) and HeLa (F) cells.

were monitored by RT-PCR. As shown in Fig. 4B, the transcription of both early and late viral genes occurred similarly in all infections.

Due to the extensive read-through that characterized transcription of late viral mRNAs, we analyzed in more detail the integrity of the A27L mRNA using primer extension analysis. As shown in Fig. 4C, the same cDNA product of 263 bp was identified using total RNAs isolated from NYVAC- and WR-infected HeLa cells. Thus, failure to produce some of the NYVAC late proteins appeared to be a consequence of a block in translation and was not due to a specific inhibition of late viral transcription.

Since it has been established that mutants of VV lacking one of the late proteins p21 (A17L), p14 (A27L), or p27.5 (L1R) are blocked at different stages in viral morphogenesis (59, 66), the absence of these proteins in NYVAC-infected cells is likely to lead to a blockade in viral morphogenesis. Thus, we next analyzed the morphogenetic process during NYVAC and MVA infection in nonpermissive cells.

Morphogenesis of NYVAC is blocked at the IV formation in HeLa-infected cells. The morphogenesis of MVA under permissive and nonpermissive conditions has been widely studied (14, 25, 42, 63, 67). The stage at which this process is blocked is dependent on the cell type. In HeLa cells, the blockade of the morphogenetic program of MVA occurs in steps following the formation of immature viral forms (IVs), without an alter-

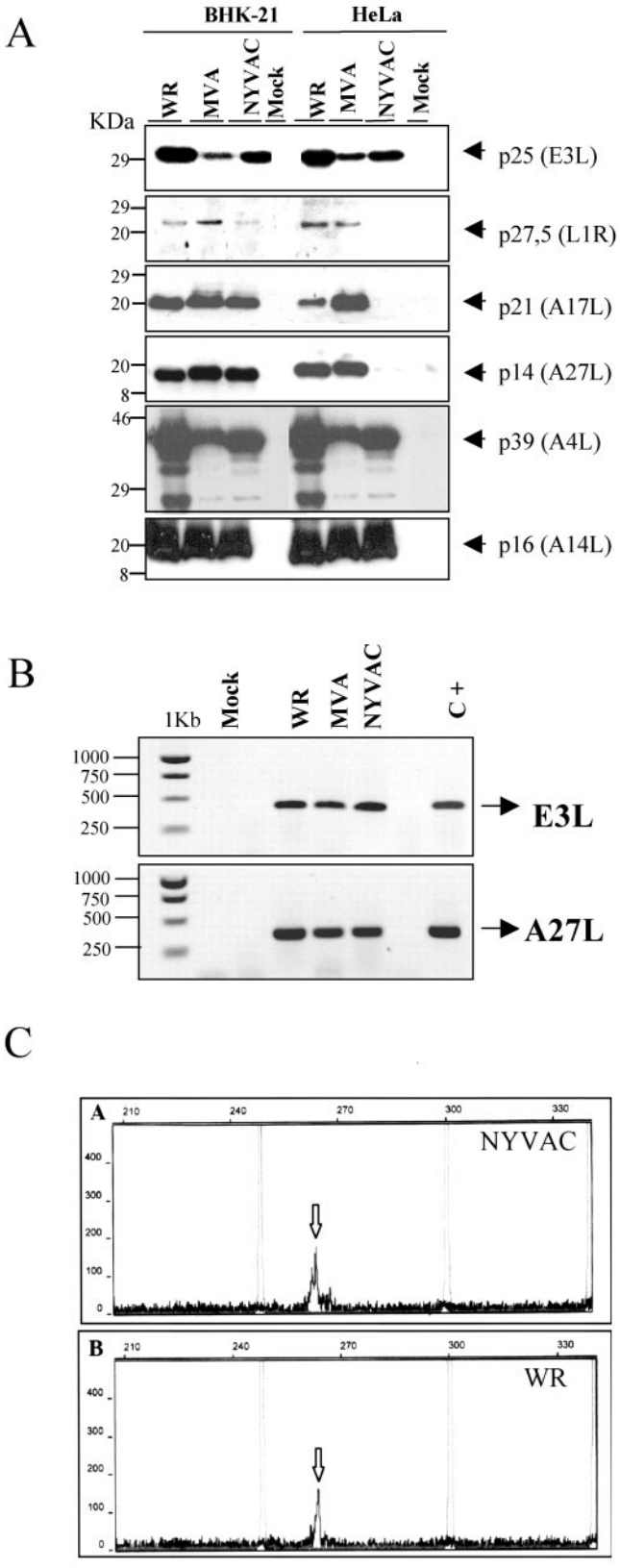

FIG. 4. Expression of specific viral proteins under permissive and nonpermissive conditions. (A) Monolayers of BHK-21 and HeLa cells were mock infected (M) or infected at 5 PFU/cell with WR, MVA, or NYVAC, and cell extracts were analyzed by Western blotting. Cell lysates were harvested at 24 h p.i., and equal amounts of proteins were fractionated by SDS-PAGE, transferred to nitrocellulose paper, and reacted with different antibodies recognizing specific viral early proteins, such as p25, and viral late proteins, such as p27.5, p21, p14, p39, or p16. (B) Transcription of early and late viral genes. The transcription of E3L and A27L genes was determined by RT-PCR from total RNAs as described in Materials and Methods. Total RNA from uninfected cells and DNA extracted from MVA-infected cells were used as the negative (Mock) and positive (C+) control, respectively. (C) Primer extension product obtained using 2 μg of total RNA isolated from HeLa cells either uninfected (Mock) or infected at 5 PFU/cell with WR or NYVAC for 16 h. The sizes of the peaks from the GeneScan-500 ROX internal lane standards are shown (in base pairs). The arrows indicate the primer extension products (VIC-labeled cDNA) for the A27L gene. Peak height is a measure of fluorescence intensity and indicates the strength of the VIC signal. The peak heights for each sample were 177 for NYVAC (A), 164 for WR (B), and 55 for mock infected (not shown).

ation in early or late viral gene expression (25, 63). In contrast, studies based on NYVAC morphogenesis are unavailable. To characterize this process under nonpermissive conditions, HeLa cells were infected at 5 PFU/cell with NYVAC or MVA. At 16 h p.i., the infected cells were examined by transmission electron microscopy for the presence of intermediates in viral morphogenesis. As shown in Fig. 5A, fewer IVs were detected in the cytoplasm of NYVAC-infected cells than in MVA-infected cells (Fig. 5B). Intracellular mature viruses were minimally detected in NYVAC-infected HeLa cells, suggesting that the blockade of the morphogenetic program of this virus occurs in steps at or prior to the formation of IVs.

Transmission electron micrographs of HeLa cells infected with NYVAC also revealed the severity of virus infection in the cell ultrastructure. As shown in Fig. 5 (panels C, D and E), morphological hallmarks of apoptosis, including chromatin condensation and margination, marked nuclear invagination, and cytoplasmic vacuolization, were observed. None of these characteristics was seen in cells infected with MVA or WR, as previously noted (25).

Infection with NYVAC induces apoptosis in human cells with activation of caspases and breakdown of rRNA. The results shown in Fig. 1 and 5 prompted us to question the extent to which NYVAC infection was responsible for an apoptotic phenotype. The cleavage of PARP commonly occurs in apoptotic cells by the activation of caspases (56). Therefore, PARP cleavage was analyzed by Western blotting of HeLa cells infected with MVA or NYVAC at different times postinfection. As shown in Fig. 6A, the 116-kDa PARP present at early times postinfection was almost completely cleaved (89 kDa) in cells infected with NYVAC at 16 h p.i. In contrast, the cleavage of PARP did not take place or was minor in MVA-infected cells. Apoptotic cells are also characterized by the presence of fragmented DNA in their nuclei. Thus, infected HeLa cells were further stained with DAPI reagent and analyzed by fluorescence microscopy. As shown in Fig. 6B, numerous HeLa nuclei displayed apoptotic morphology (chromatin condensation and disintegration) at 24 h p.i. in cells infected with NYVAC. In contrast, a very low percentage of all the cells infected with MVA presented this phenotype. These results were further supported by an enzyme-linked immunosorbent assay-based

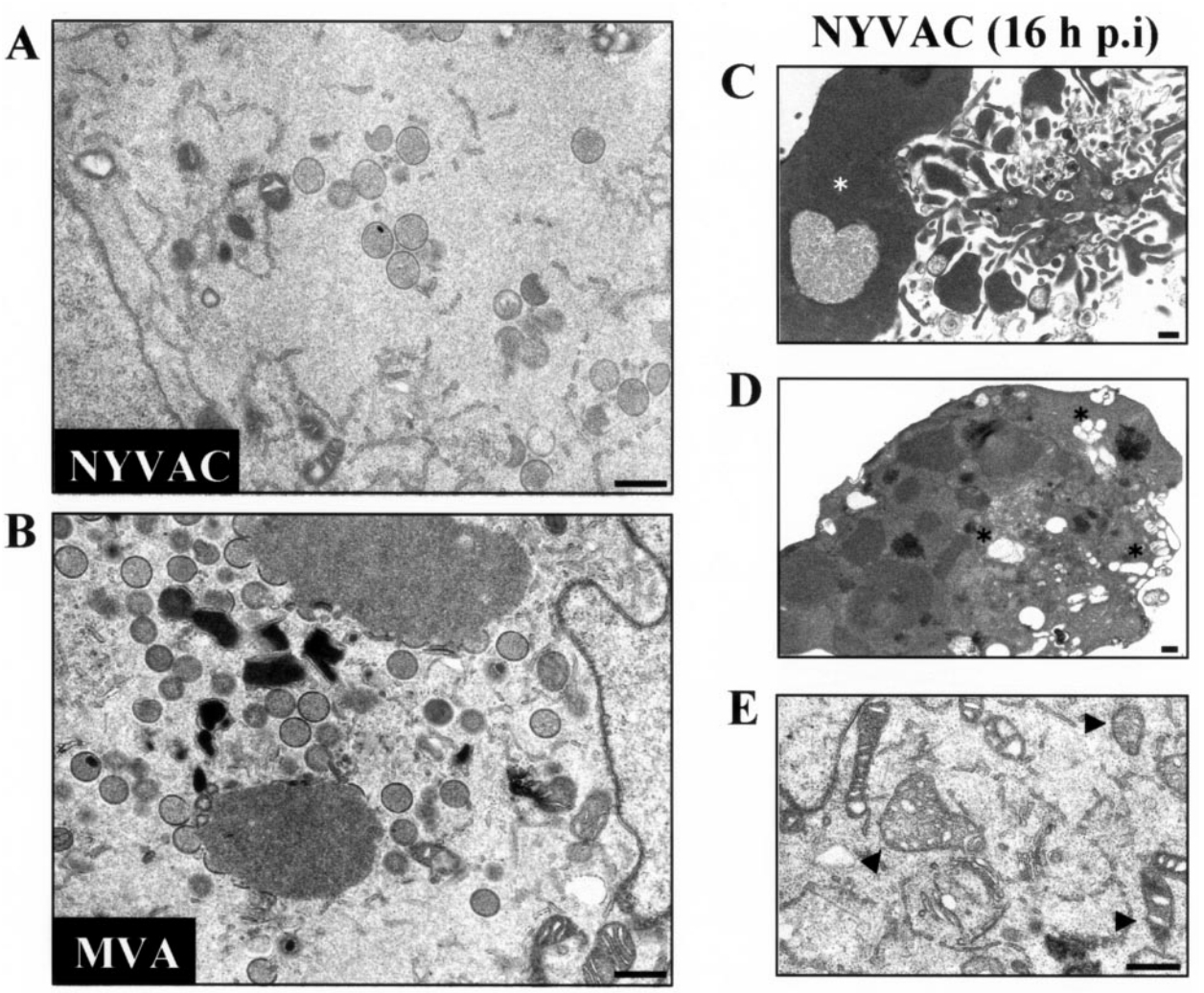

FIG. 5. Electron microscopy of NYVAC morphogenesis in HeLa cells. (A and B) Electron micrographs of HeLa cells infected with 5 PFU/cell of NYVAC (A) or with 5 PFU/cell of MVA (B) at 16 h p.i. The magnification of each panel is indicated by bars in the upper right corner. Characteristics of apoptosis in NYVAC-infected cells are shown in panels C to E. (C) An infected cell with nuclear condensation (white asterisk). (D) Cytoplasm of an infected cell with extensive vacuolation (black asterisks). (E) Cytoplasm of an infected cell with dense mitochondria (arrowheads). Bars = 500 nm.

assay that detects the amount of cytoplasmic histone-associated DNA fragments (data not shown).

To quantify the percentage of cell death following infection, we used flow cytometry. When these cells are stained with propidium iodide, apoptotic cells show reduced levels of fluorescence compared to normal cells and appear in the sub-G_0/G_1 peak (18). Thus, HeLa cells were infected at 5 PFU/cell with WR, MVA, or NYVAC in the presence or absence of zVAD (a general caspase inhibitor). At 24 h p.i., the infected cells were stained with propidium iodide followed by cell cycle analysis using flow cytometry. Mock-infected HeLa cells were used as a negative control. As shown in Fig. 6C, approximately 42% of cells infected with NYVAC were present in the sub-G_0/G_1 peak, which represents an increase of nearly sevenfold with respect to uninfected cells, in comparison with the 17.6% and 9.3% obtained in MVA- or WR-infected cells, respectively. In the presence of zVAD, the percentage of apoptotic cells was significantly reduced (3.67%), demonstrating that the apoptosis induced by NYVAC infection is caspase dependent.

The activation of nucleases appears to be a final commitment step in the apoptotic process. Thus, we next examined the effect of nuclease activation on rRNA integrity. Total RNA was isolated from infected and mock-infected cells and fractionated by formaldehyde-agarose gel electrophoresis. As shown in Fig. 6D, the bands corresponding to 28S and 18S rRNA were intact in those samples from mock-, WR-, or MVA-infected cells. In contrast, in NYVAC-infected cells there was breakdown of rRNA. The rRNA fragments generated by NYVAC infection were similar to those produced after activation of the enzyme RNase L (not shown). Clearly, by 24 h p.i. NYVAC induces severe rRNA cleavage. These biochemical findings indicate a remarkable apoptotic process during NYVAC infection.

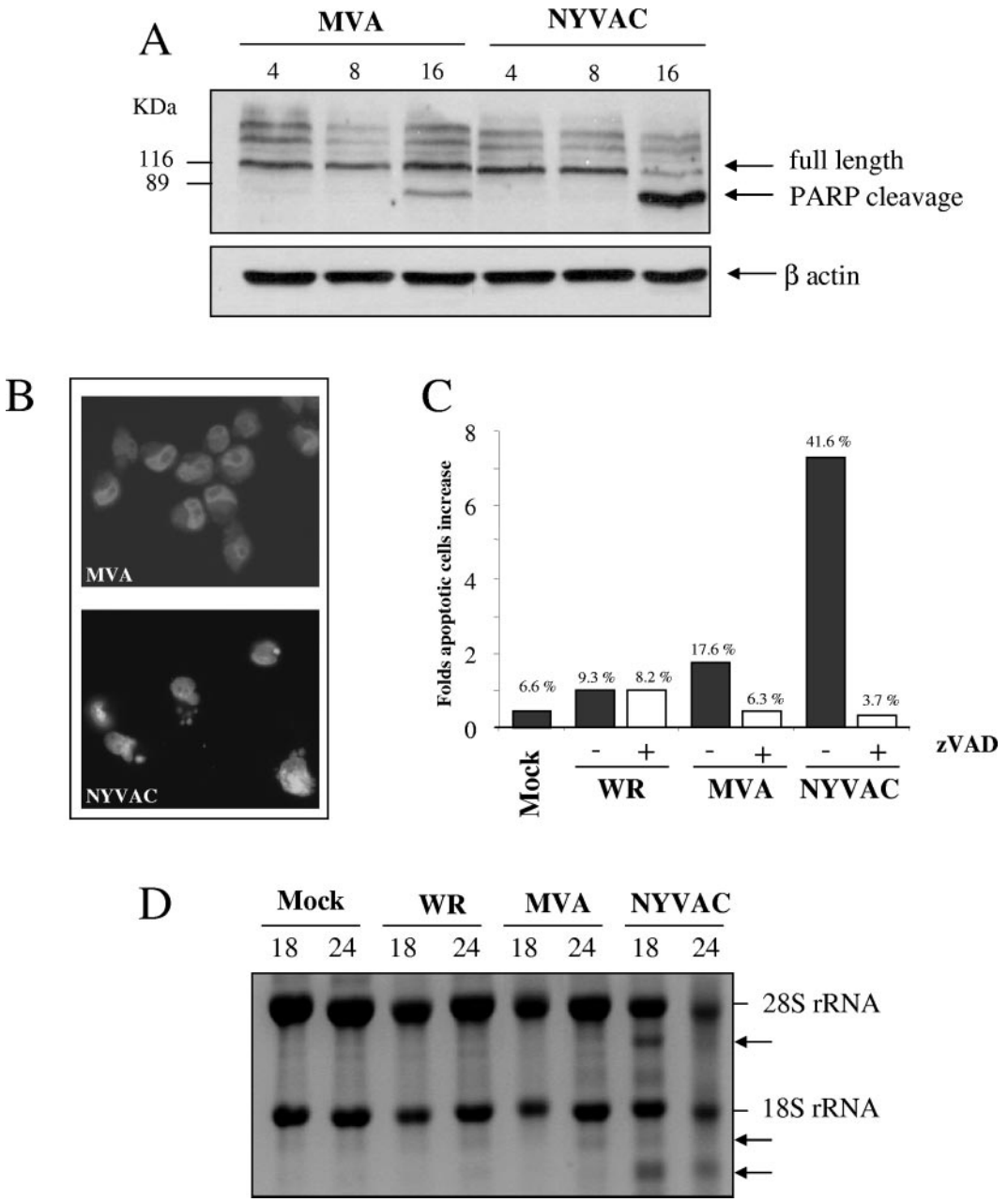

FIG. 6. Infection with NYVAC induces apoptosis in nonpermissive HeLa cells. (A) Western blot analysis of PARP cleavage in HeLa cells infected with 5 PFU/cell of MVA or NYVAC at different times postinfection. (B) DAPI staining of HeLa cells infected with 5 PFU/cell of MVA and NYVAC at 24 h p.i. (C) Monolayers of HeLa cells were infected at 5 PFU/cell with WR, MVA, or NYVAC in the presence or absence of zVAD (40 μM). At 24 h p.i., the infected cells were stained with propidium iodide followed by cell cycle analysis using a flow cytometer to detect cells with hypodiploid DNA content. Untreated HeLa cells were used as a negative control (Mock). Bars represent the fold increase in apoptotic cells with respect to mock infected. The percentage of apoptotic cells is indicated over the bars. Similar results were obtained in two independent experiments. (D) rRNA breakdown. HeLa cells were mock infected or infected with WR, MVA, or NYVAC at 5 PFU/cell. Total RNA was isolated at 18 and 24 h p.i., and 2 μg of each was applied for electrophoresis. The arrows indicate bands corresponding to characteristic degradation products of rRNA.

The viral C7L gene blocked apoptosis induced by NYVAC infection and rescued the biological and biochemical properties assigned to NYVAC. Critical parts of the cellular antiviral response range from the induction of apoptosis and the global inhibition of translation to effectively dampening virus production (64). Since NYVAC was generated by target deletion of 18 genes, including the host range (Hr) gene C7L, and Hr genes have been implicated in apoptosis (74), it was of interest to know whether reintroduction of C7L in the NYVAC genome could rescue some of the biological properties of NYVAC assigned in this study. To this aim, the C7L gene from MVA was used for the generation of the recombinant virus NYVAC-C7L. Because our data demonstrated that NYVAC infection triggered programmed cell death in HeLa cells, we asked

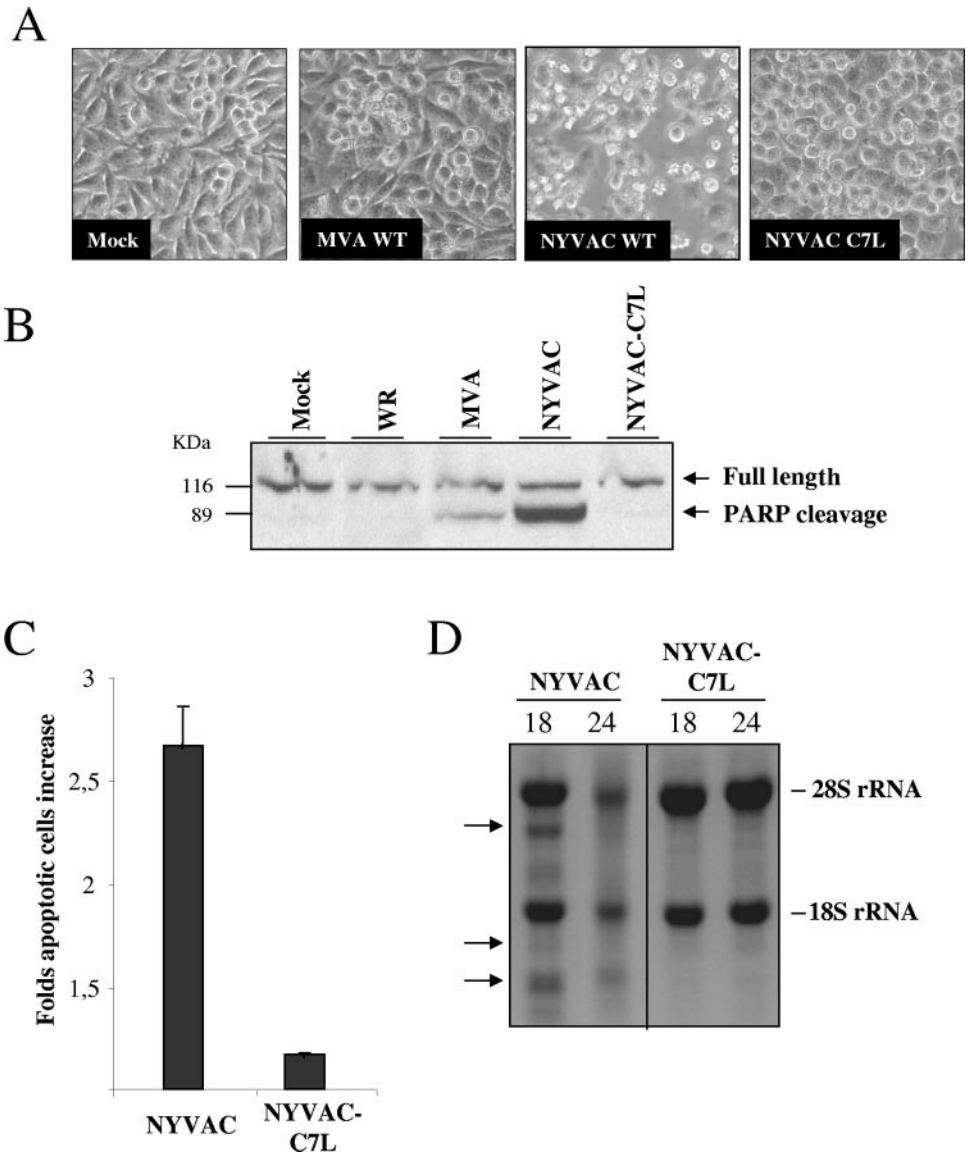

FIG. 7. The apoptotic phenotype of NYVAC is inhibited by the expression of the virus C7L host range gene. Monolayers of HeLa cells were infected with recombinant NYVAC-C7L or with MVA or the NYVAC wild type (WT) at 5 PFU/cell. (A) The morphology of cells in apoptosis was observed by phase-contrast microscopy. (B) Western blot analysis of PARP cleavage in HeLa cells infected with WR, MVA, NYVAC, or NYVAC-C7L at 24 h p.i. (C) Monolayers of HeLa cells were infected at 5 PFU/cell with NYVAC or NYVAC-C7L. At 24 h p.i., the infected cells were stained with propidium iodide followed by cell cycle analysis using a flow cytometer to detect cells with hypodiploid DNA. Uninfected HeLa cells (Mock) were used as a negative control. Bars represent the fold increase in apoptotic cells with respect to mock infected. (D) rRNA breakdown. HeLa cells were infected with NYVAC or NYVAC-C7L at 5 PFU/cell. Total RNA was isolated at 18 and 24 h p.i., and 2 μg of each was applied for electrophoresis. The arrows indicate bands corresponding to characteristic degradation products of rRNA.

whether NYVAC-C7L was capable of inhibiting apoptosis. We monitored apoptosis by assessing morphological changes, cleavage of PARP, rRNA degradation, and cell cycle assays. The morphological signs of apoptosis observed in NYVAC-infected HeLa cells were not evident after infection with NYVAC-C7L (Fig. 7A). In addition, the recombinant virus was able to prevent cleavage of PARP (Fig. 7B), reduced the percentage of cells in apoptosis (Fig. 7C), and inhibited the breakdown of rRNA (Fig. 7D). These observations clearly revealed that the C7L gene is involved in the control of apoptosis induced by NYVAC infection. Since during NYVAC infection the enhanced shutoff correlated with eIF2-α phosphorylation, we next investigated the role of C7L in translational control by measuring phosphorylation of eIF2-α and expression of p14 (A27L) and p21 (A17L) late viral proteins. As shown in Fig. 8A, in NYVAC-C7L-infected HeLa cells there was rescue in the synthesis of late viral proteins (p14 and p21) at 24 h p.i. compared with parental NYVAC infection and the levels of phosphorylated eIF2-α were similar to those in MVA-infected cells. This rescue in the synthesis of late viral proteins is likely to favor virus replication in the human cells. Thus, the viral growth efficiency of NYVAC-C7L in HeLa cells was measured. Monolayers of HeLa cells were infected at 0.01 PFU/cell with NYVAC or NYVAC-C7L, and at times 0, 24,

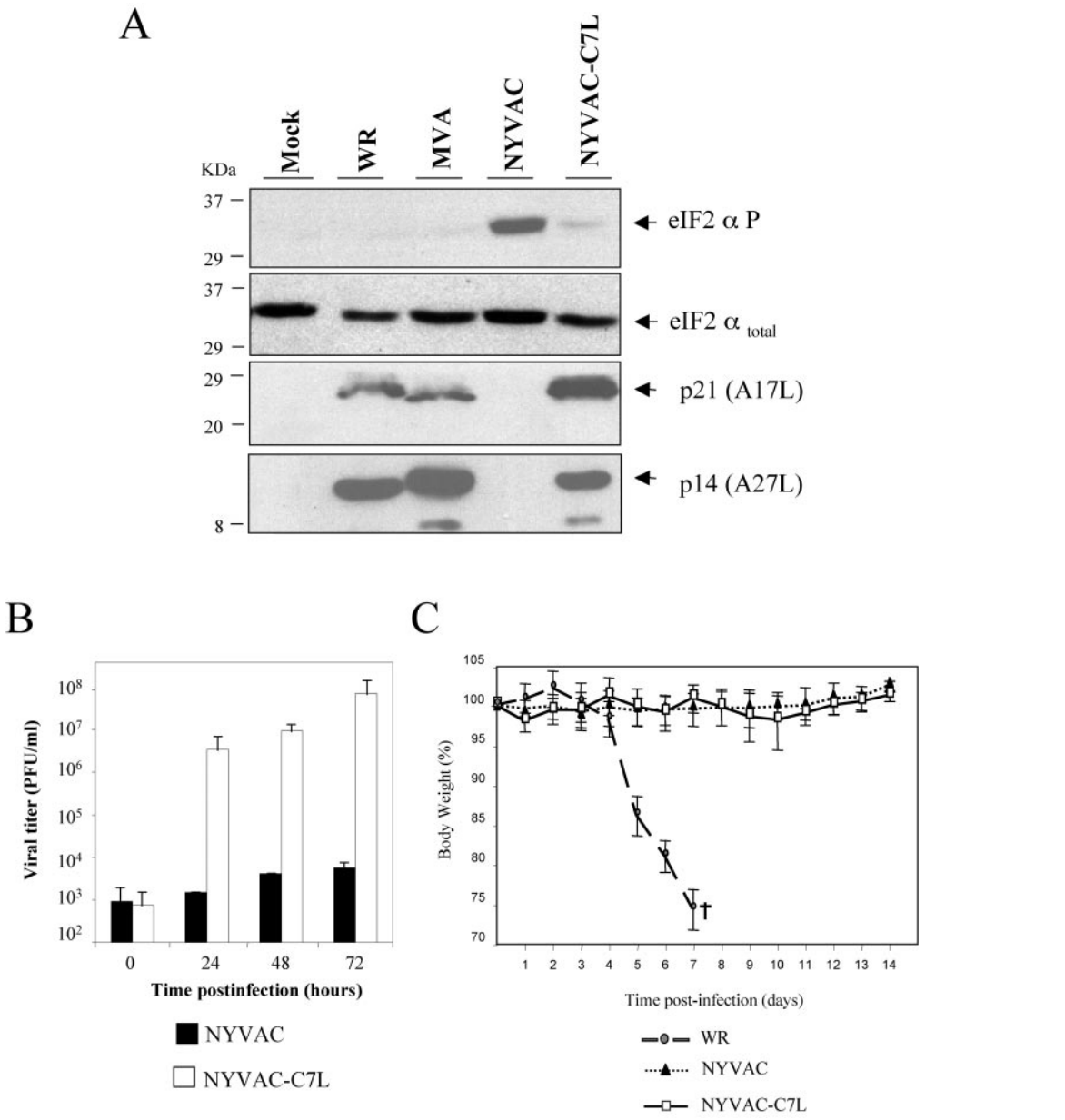

FIG. 8. The VV C7L gene rescued NYVAC translation capacity and virus growth in human cells but retained the attenuated phenotype in vivo. (A) Expression of total and phospho-eIF2-α and late viral proteins (p21 and p14) in HeLa cells uninfected (Mock) or infected with 5 PFU/cell of WR, MVA, NYVAC, or NYVAC-C7L at 24 h p.i. was analyzed by Western blotting. (B) Monolayers of HeLa cells were infected at 0.01 PFU/cell with NYVAC or NYVAC-C7L virus for 0, 24, 48, and 72 h. Cells were collected by centrifugation, and infectious virus associated with the cells during the course of the infection was quantified by immunostaining assay. Two independent experiments are shown with standard error bars. (C) BALB/c mice ($n = 4$) were inoculated by the i.n. route with different challenge doses of either NYVAC or NYVAC-C7L (from 10^6 to 10^8 PFU/mouse) or with 10^6 PFU/mouse of WR. Body weight was monitored daily and is expressed as the mean for each group. Animals suffering from severe systemic infection and having lost >25% body weight were sacrificed (black cross). The graph represents the values obtained using the highest dose of NYVAC and NYVAC-C7L (10^8 PFU/mouse) and the low dose (10^6 PFU/mouse) of WR.

48, and 72 h, cells were collected in the media and virus titers in cell homogenates were determined by immunostaining assay. As shown in Fig. 8B, reintroduction of the C7L gene in the NYVAC genome rescues the ability of this virus to replicate in HeLa cells. To define if the introduction of the C7L gene in NYVAC alters the attenuated phenotype of the virus, BALB/c mice were infected by the i.n. route with different challenge doses of NYVAC or NYVAC-C7L (from 10^6 to 10^8 PFU/mouse) or with 10^6 PFU of WR as a control. Animals were monitored for lethality and weight loss over a period of 2 weeks. In contrast to WR infection, which caused drastic body weight loss and severe signs of illness, infection of mice with NYVAC or with the recombinant NYVAC-C7L did not lead to any obvious disease, even at the highest dose used (Fig. 8C). These results revealed that reintroduction of the C7L gene into the backbone of NYVAC maintains an attenuated phenotype of the recombinant virus. Thus, the findings of Fig. 7 and 8 demonstrate that most, if not all, of the biological and bio-

chemical features of NYVAC infection that we have observed in this study are largely due to the lack of the C7L gene.

DISCUSSION

There is major interest in the use of poxviruses as vaccine vectors and as oncolytic agents against a broad spectrum of diseases, due to their ability to trigger specific immune responses leading to protection in animal models and their capacity to destroy tumor cells (24, 41). Live attenuated strains, such as MVA, NYVAC, ALVAC, and fowlpox virus, which have been modified to be less virulent and to exhibit a specific phenotype, are the most extensively studied vectors. The rational design of such vaccines requires detailed information on vector-host cell interactions and how viral genomic modifications impact the biology and immunogenicity of the poxvirus vectors (35). Currently, a number of clinical trials are under way by EuroVacc (www.eurovacc.org) as well as other organizations with the two attenuated poxvirus vectors NYVAC and MVA (8, 9). As such, it is crucial to understand the behavior of the two vectors in both in vitro and in vivo systems. In this work, we carried out an in vitro head-to-head comparison of the cellular and biochemical properties between NYVAC and MVA in nonpermissive and permissive cultured cells.

Several biological differences between both strains in vitro were evident. The first significant difference involves the CPE produced by NYVAC compared with WR and MVA strains. This CPE was observed early in NYVAC infection in a range of permissive and nonpermissive cell lines, indicating that CPE is independent of the host range restriction and was maintained even when DNA replication was blocked by the drug Ara C. As reported by previous authors, the induction of early cell rounding is dependent on early viral protein synthesis (2, 3, 5). Consequently, Tsung and coworkers demonstrated the absence of CPE in cells infected with a VV strain inactivated by psoralen and long-wave UV light, a treatment that affects the transcription of early viral genes (73). Although WR and NYVAC induced a similar CPE at early times postinfection from 2 to 6 h p.i., NYVAC-infected cells displayed a more pronounced cell rounding than WR-infected cells. The CPE induced by MVA was minor compared to those induced by WR and NYVAC. The reduced CPE by MVA may be attributed to the fact that MVA has lost 15% of its parental genome and could be related to the absence of some early viral proteins encoded by the deleted genes. We discard the possibility that these effects could be due to differences in the number of virus particles used to infect cells, since the particle/PFU ratios for the three virus preparations were similar.

The second significant difference between NYVAC and MVA includes the amount of virus that remains cell associated late in infection. As has been shown by other studies, the growth of MVA (14, 20) and NYVAC (69) is restricted in HeLa cells; however, both strains can be grown in BHK-21 cells. Interestingly, as shown here, the titers of cell-associated virus in BHK-21 cells infected with NYVAC were consistently lower than the titers obtained in cells infected with WR or MVA. This result might be linked with the pronounced CPE induced in NYVAC-infected cells, as the structures of some organelles involved in virus morphogenesis, such as the Golgi apparatus, were altered at early times postinfection. The lower cell-associated viral yields obtained in NYVAC-infected cells under permissive conditions could explain the difficulties encountered by Gonin and coworkers in producing high titers of a NYVAC recombinant (28).

A third significant difference observed between NYVAC and MVA infection was in the synthesis of viral proteins and the extent of phosphorylation of the translational initiation factor eIF-2α. In permissive and nonpermissive cell lines, NYVAC infection produces a reduction in the kinetics of synthesis and accumulation of viral proteins with time. Inhibition of protein synthesis during NYVAC infection was associated with an increase in the phospho-eIF-2α-S51 levels. Since eIF-2α is a key regulator of translation, our observations imply that protein synthesis is more compromised during NYVAC than MVA infection. Consequently, certain late viral proteins such as p14 (A27L), p21 (A17L), or the L1R gene product (p27.5) were not detected in nonpermissive cells infected with NYVAC, while other late viral proteins required for early steps in morphogenesis (59), such as p16 (A14L) or p39 (A4L), were synthesized. The lack of synthesis of some late viral proteins was not due to inhibition of transcription of these genes but rather to a block at the translational level, as revealed by the integrity of mRNAs for these genes in NYVAC-infected cells determined by RT-PCR and primer extension (Fig. 4). The fact that such proteins were not detected in cell lines in which NYVAC growth was restricted (mouse 3T3 and human TK-143 cells; data not shown), indicates that it is a feature of the host restriction of this attenuated strain. Nonetheless, we cannot exclude the possibility that trace amounts of these proteins may be synthesized but are not detected by Western blotting or by immunofluorescence analysis. These findings could be considered promising with regards to the safety of NYVAC, since the virus is unable to synthesize the late viral proteins needed for the correct assembly and formation of infectious viral particles under nonpermissive conditions.

A fourth variation obtained between MVA and NYVAC infection is based on morphogenesis. The stage of infection in which the block in the viral life cycle of both strains occurs is dependent on the cell type. In cell lines of human origin such as HeLa, MVA infection is blocked at late times postinfection, while early and late viral protein syntheses are produced like in permissive cells; MVA assembly is inhibited after IV formation (25, 63, 67). In the case of NYVAC-infected HeLa cells, the block in morphogenesis occurs at or prior to the formation of IVs. This block could be related to the absence of certain late structural proteins required for morphogenesis. Although this study examined a limited number of late proteins, it is important to note that some of the late proteins required for virus assembly (59, 66), including p21 (A17L) and p27.5 (L1R), are not produced or are produced minimally in NYVAC-infected cells. Translational inhibition in the synthesis of some of the late viral proteins in NYVAC-infected human cells could occur at two levels. As shown here, NYVAC infection was associated with an increase in the phospho-eIF-2α-S51 levels and with rRNA breakdown. The rRNA cleavage fragments were similar in size to those produced after activation of the cellular RNase L enzyme (not shown), indicating that NYVAC infection triggered RNase L function. It is well established that eIF-2 phosphorylation and rRNA cleavage are two pathways that play a critical role in the antiviral response of interferons and are

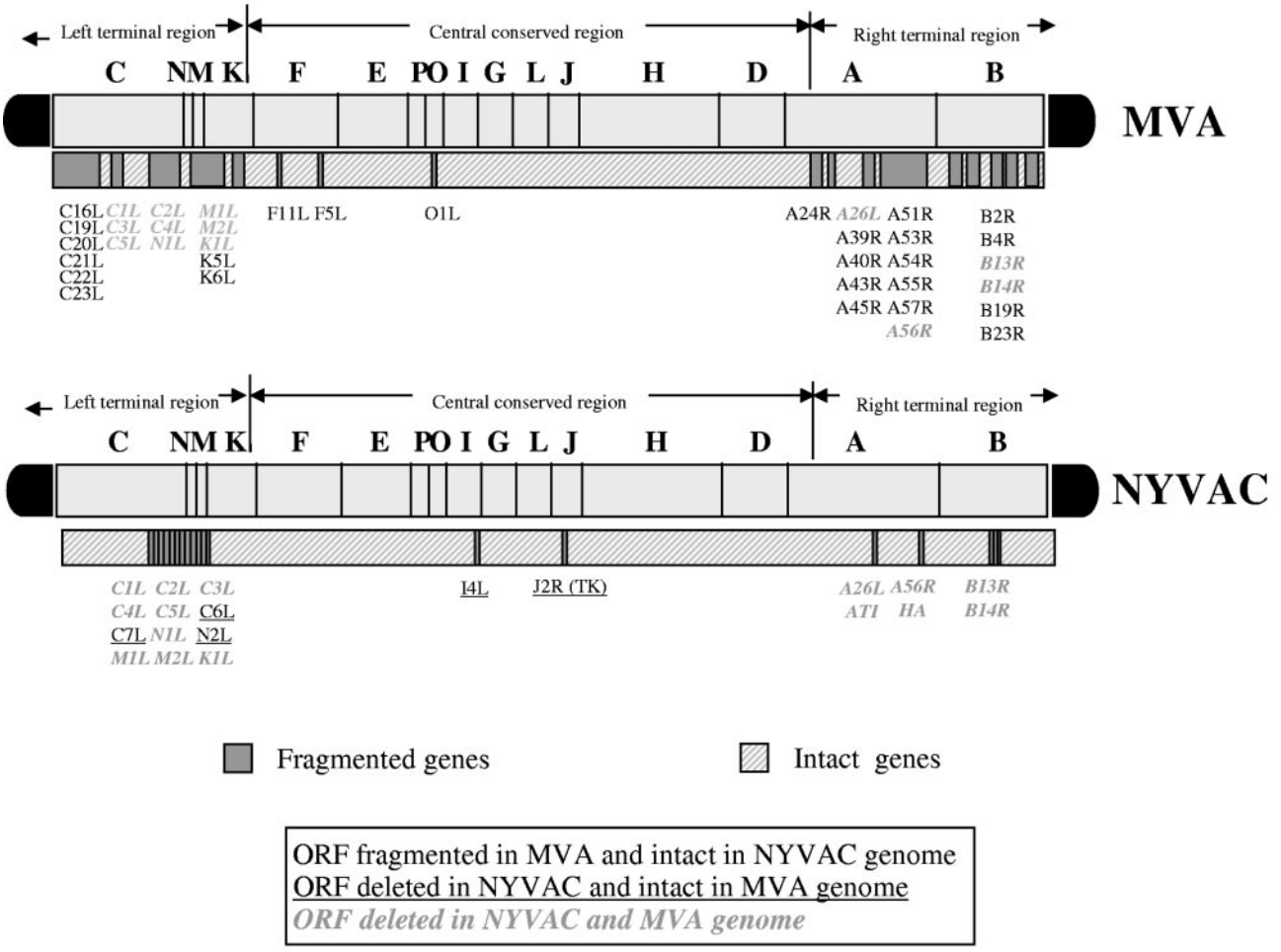

FIG. 9. Scheme of deleted genes in MVA and NYVAC genomes. Genome maps of MVA and NYVAC strains adapted from Antoine et al. (1) are represented. The deleted or fragmented genes in each genome are indicated. The right and left terminal regions are shown.

activated by double-stranded RNA (dsRNA) (64, 77). Since RNA breakdown should not discriminate between different mRNAs in the cytoplasm of the cell, local activation of eIF-2 phosphorylation could, in turn, be responsible for the apparent selective block in translation of some late viral proteins. As yet, it has not been explored whether there is specificity in translation of late viral mRNAs at focal sites in the cell cytoplasm, and the NYVAC-infected cell system could provide the means to unravel translational selectivity.

A fifth important difference observed between MVA and NYVAC was related to apoptosis. Upon infection with NYVAC, HeLa cells display morphological and biochemical features typical of apoptosis. In addition to the characteristic morphological hallmarks of programmed cell death observed by electron and light microscopy in NYVAC infection, and not in MVA, biochemical parameters such us PARP cleavage or DNA fragmentation were also evident. Flow cytometry analysis of cells infected with MVA and NYVAC that had been stained with propidium iodide revealed that the percentage of apoptotic cells in MVA infection was significantly lower than in NYVAC infection. Nearly 42% of NYVAC-infected cells demonstrated an apoptotic phenotype by 24 h p.i. Furthermore, these percentages were reduced to background levels when infected cells were treated with zVAD, a general caspase inhibitor, indicating that the apoptosis induced by NYVAC infection is caspase dependent.

Since apoptosis is an important mechanism for limiting virus infection, it is not surprising that poxviruses encode certain proteins to counteract the cell death phenomenon (7, 41, 65, 74). Some of the genes coding for these proteins critical for the control of apoptosis, such as the serpin homologs encoded by the gene B14R or B13R (the corresponding homologs of the Copenhagen VV strain referred as MVA182R and 181R), are deleted in both MVA and NYVAC (1, 36, 76). Other gene products known to block apoptosis are encoded by E3L (MVA050L) (acting through sequestration of dsRNA and prevention of activation of PKR and the 2-5A system) (16, 26, 58) and by F1L (MVA029L), an inhibitor of the mitochondrial caspase 9-induced apoptosis (75). Both genes E3L and F1L are present in NYVAC and MVA. Antoine and coworkers (1) compared the genomes of MVA and NYVAC and their respective deleted genes, which is detailed in Fig. 9. A comparison between MVA and NYVAC revealed that both viruses share common deleted or nonfunctional open reading frames (ORFs), including the six ORFs within the deletion d4817 (C5L-N1L), ORFs B13R and B14R encoding the ICE inhibi-

tor, the ATI remnant ORF A26L, and the K1L (MVA022L) host range gene. In contrast to NYVAC, the MVA strain has a functional thymidine kinase gene (TK), an intact C7L (MVA018L) host range gene, and intact C6L (MVA019L), A56R (MVA165R), N2L (MVA021L), and I4L (MVA065L) ORFs. This suggests that some of these genes might be involved in the differential NYVAC in vitro behavior with respect to MVA. As has been reported by others, the host range genes for VV C7L, K1L, and cowpox virus CP77 in some cell lines (including HeLa cells) behaved as equivalent genes, even in the absence of amino acid similarity. Thus, deletion of one host gene could be compensated for by the presence of another, suggesting that these host range genes act in common pathways (34, 51, 54, 55). As shown here, the viral C7L gene plays a critical role in apoptosis induced by NYVAC infection as well as in many of the biological and biochemical features described in this work for NYVAC. When the C7L gene was reintroduced into the NYVAC genome, the recombinant NYVAC-C7L virus lost the ability to trigger apoptosis, to induce eIF-2α phosphorylation, and to activate rRNA breakdown, and in turn it rescued the translation capacity of late viral mRNAs and of virus multiplication in human cells. Significantly, the recombinant NYVAC-C7L virus maintains an in vivo attenuated phenotype. The fact that the C7L gene is well conserved in all of the orthopoxvirus genomes that have been sequenced highlights the importance of this gene in virus biology by counteracting host responses (29).

The head-to-head comparative analysis performed in this study between MVA and NYVAC not only will be a crucial basis for eventual prioritization of the most promising vaccine candidates based on these vectors, but also will be of great significance to vaccine research for the development of new innovative poxvirus vectors for clinical testing, providing enhanced immune responses to the foreign antigen by deletions and/or additions of immunomodulators. This approach must be applied and extended to the comparative analysis of the different immune responses produced by recombinants based on MVA or NYVAC strains. Mouse, monkey, and clinical studies of head-to-head comparison between NYVAC and MVA expressing the same cassette of HIV genes are under way by EuroVacc (www.eurovacc.org). Undoubtedly, the differential behavior observed in this study between NYVAC and MVA could play a role in the magnitude and extent of immune responses triggered by these vectors when applied for vaccination purposes.

ACKNOWLEDGMENTS

This investigation was supported by research grants from the Spanish Ministry of Education and Science BIO2004-03954, the Spanish Foundation for AIDS Research (FIPSE 36344/02), Fundación Marcelino Botín, and the EU (EuroVac QLRT-PL-1999-01321 and QLK2-CT-2002-01867). C. E. Gómez was the recipient of a Fundación Carolina fellowship, and J. L. Nájera was supported by FIPSE.

We thank Victoria Jiménez, C. Patiño, and Sylvia Gutiérrez for expert technical assistance and Patricia Martínez for editorial assistance. We are grateful to J. Tartaglia (Aventis-Pasteur) for generously providing the NYVAC strain.

REFERENCES

1. **Antoine, G., F. Scheiflinger, F. Dorner, and F. G. Falkner.** 1998. The complete genomic sequence of the modified vaccinia Ankara strain: comparison with other orthopoxviruses. Virology **244:**365–396.
2. **Bablanian, R., B. Baxt, J. A. Sonnabend, and M. Esteban.** 1978. Studies on the mechanisms of vaccinia virus cytopathic effects. II. Early cell rounding is associated with virus polypeptide synthesis. J. Gen. Virol. **39:**403–413.
3. **Bablanian, R., G. Coppola, S. Scribani, and M. Esteban.** 1981. Inhibition of protein synthesis by vaccinia virus. III. The effect of ultraviolet-irradiated virus on the inhibition of protein synthesis. Virology **112:**1–12.
4. **Bablanian, R., G. Coppola, S. Scribani, and M. Esteban.** 1981. Inhibition of protein synthesis by vaccinia virus. IV. The role of low-molecular-weight viral RNA in the inhibition of protein synthesis. Virology **112:**13–24.
5. **Bablanian, R., M. Esteban, B. Baxt, and J. A. Sonnabend.** 1978. Studies on the mechanisms of vaccinia virus cytopathic effects. I. Inhibition of protein synthesis in infected cells is associated with virus-induced RNA synthesis. J. Gen. Virol. **39:**391–402.
6. **Bablanian, R., S. K. Goswami, M. Esteban, and A. K. Banerjee.** 1987. Selective inhibition of protein synthesis by synthetic and vaccinia virus core synthesized poly(riboadenylic acids). Virology **161:**366–373.
7. **Barry, M., S. T. Wasilenko, T. L. Stewart, and J. M. Taylor.** 2004. Apoptosis regulator genes encoded by poxviruses. Prog. Mol. Subcell. Biol. **36:**19–37.
8. **Bayes, M., X. Rabasseda, and J. R. Prous.** 2005. Gateways to clinical trials. Methods Find. Exp. Clin. Pharmacol. **27:**193–219.
9. **Bayes, M., X. Rabasseda, and J. R. Prous.** 2005. Gateways to clinical trials. Methods Find. Exp. Clin. Pharmacol. **27:**49–77.
10. **Belyakov, I. M., P. Earl, A. Dzutsev, V. A. Kuznetsov, M. Lemon, L. S. Wyatt, J. T. Snyder, J. D. Ahlers, G. Franchini, B. Moss, and J. A. Berzofsky.** 2003. Shared modes of protection against poxvirus infection by attenuated and conventional smallpox vaccine viruses. Proc. Natl. Acad. Sci. USA **100:**9458–9463.
11. **Blasco, R., and B. Moss.** 1991. Extracellular vaccinia virus formation and cell-to-cell virus transmission are prevented by deletion of the gene encoding the 37,000-dalton outer envelope protein. J. Virol. **65:**5910–5920.
12. **Brockmeier, S. L., and W. L. Mengeling.** 1996. Comparison of the protective response induced by NYVAC vaccinia recombinants expressing either gp50 or gII and gp50 of pseudorabies virus. Can. J. Vet. Res. **60:**315–317.
13. **Broyles, S. S.** 2003. Vaccinia virus transcription. J. Gen. Virol. **84:**2293–2303.
14. **Carroll, M. W., and B. Moss.** 1997. Host range and cytopathogenicity of the highly attenuated MVA strain of vaccinia virus: propagation and generation of recombinant viruses in a nonhuman mammalian cell line. Virology **238:**198–211.
15. **Carroll, M. W., W. W. Overwijk, R. S. Chamberlain, S. A. Rosenberg, B. Moss, and N. P. Restifo.** 1997. Highly attenuated modified vaccinia virus Ankara (MVA) as an effective recombinant vector: a murine tumor model. Vaccine **15:**387–394.
16. **Chang, H. W., J. C. Watson, and B. L. Jacobs.** 1992. The E3L gene of vaccinia virus encodes an inhibitor of the interferon-induced, double-stranded RNA-dependent protein kinase. Proc. Natl. Acad. Sci. USA **89:**4825–4829.
17. **Dallo, S., J. F. Rodriguez, and M. Esteban.** 1987. A 14K envelope protein of vaccinia virus with an important role in virus-host cell interactions is altered during virus persistence and determines the plaque size phenotype of the virus. Virology **159:**423–432.
18. **Darzynkiewicz, Z., S. Bruno, G. Del Bino, W. Gorczyca, M. A. Hotz, P. Lassota, and F. Traganos.** 1992. Features of apoptotic cells measured by flow cytometry. Cytometry **13:**795–808.
19. **Didierlaurent, A., J. C. Ramirez, M. Gherardi, S. C. Zimmerli, M. Graf, H. A. Orbea, G. Pantaleo, R. Wagner, M. Esteban, J. P. Kraehenbuhl, and J. C. Sirard.** 2004. Attenuated poxviruses expressing a synthetic HIV protein stimulate HLA-A2-restricted cytotoxic T-cell responses. Vaccine **22:**3395–3403.
20. **Drexler, I., K. Heller, B. Wahren, V. Erfle, and G. Sutter.** 1998. Highly attenuated modified vaccinia virus Ankara replicates in baby hamster kidney cells, a potential host for virus propagation, but not in various human transformed and primary cells. J. Gen. Virol. **79:**347–352.
21. **Drexler, I., C. Staib, and G. Sutter.** 2004. Modified vaccinia virus Ankara as antigen delivery system: how can we best use its potential? Curr. Opin. Biotechnol. **15:**506–512.
22. **Esteban, M.** 1984. Defective vaccinia virus particles in interferon-treated infected cells. Virology **133:**220–227.
23. **Franchini, G., J. Benson, R. Gallo, E. Paoletti, and J. Tartaglia.** 1996. Attenuated poxvirus vectors as carriers in vaccines against human T cell leukemia-lymphoma virus type I. AIDS Res. Hum. Retrovir. **12:**407–408.
24. **Franchini, G., S. Gurunathan, L. Baglyos, S. Plotkin, and J. Tartaglia.** 2004. Poxvirus-based vaccine candidates for HIV: two decades of experience with special emphasis on canarypox vectors. Expert Rev. Vaccines **3:**S75–S88.
25. **Gallego-Gómez, J. C., C. Risco, D. Rodriguez, P. Cabezas, S. Guerra, J. L. Carrascosa, and M. Esteban.** 2003. Differences in virus-induced cell morphology and in virus maturation between MVA and other strains (WR, Ankara, and NYCBH) of vaccinia virus in infected human cells. J. Virol. **77:**10606–10622.
26. **Garcia, M. A., S. Guerra, J. Gil, V. Jimenez, and M. Esteban.** 2002. Anti-apoptotic and oncogenic properties of the dsRNA-binding protein of vaccinia virus, E3L. Oncogene **21:**8379–8387.
27. **Gherardi, M. M., J. C. Ramirez, D. Rodriguez, J. R. Rodriguez, G. Sano, F. Zavala, and M. Esteban.** 1999. IL-12 delivery from recombinant vaccinia virus

attenuates the vector and enhances the cellular immune response against HIV-1 Env in a dose-dependent manner. J. Immunol. **162:**6724–6733.
28. **Gonin, P., W. Oualikene, A. Fournier, and M. Eloit.** 1996. Comparison of the efficacy of replication-defective adenovirus and Nyvac poxvirus as vaccine vectors in mice. Vaccine **14:**1083–1087.
29. **Gubser, C., S. Hue, P. Kellam, and G. L. Smith.** 2004. Poxvirus genomes: a phylogenetic analysis. J. Gen. Virol. **85:**105–117.
30. **Guerra, S., L. A. López-Fernández, R. Conde, A. Pascual-Montano, K. Harshman, and M. Esteban.** 2004. Microarray analysis reveals characteristic changes of host cell gene expression in response to attenuated modified vaccinia virus Ankara infection of human HeLa cells. J. Virol. **78:**5820–5834.
31. **Guerra, S., L. A. López-Fernández, A. Pascual-Montano, J. L. Nájera, A. Zaballos, and M. Esteban.** 2006. Host response to the attenuated poxvirus vector NYVAC: upregulation of apoptotic genes and NF-κB-responsive genes in infected HeLa cells. J. Virol. **80:**985–998.
32. **Hel, Z., J. Nacsa, W. P. Tsai, A. Thornton, L. Giuliani, J. Tartaglia, and G. Franchini.** 2002. Equivalent immunogenicity of the highly attenuated poxvirus-based ALVAC-SIV and NYVAC-SIV vaccine candidates in SIVmac251-infected macaques. Virology **304:**125–134.
33. **Hornemann, S., O. Harlin, C. Staib, S. Kisling, V. Erfle, B. Kaspers, G. Hacker, and G. Sutter.** 2003. Replication of modified vaccinia virus Ankara in primary chicken embryo fibroblasts requires expression of the interferon resistance gene E3L. J. Virol. **77:**8394–8407.
34. **Hsiao, J. C., C. S. Chung, R. Drillien, and W. Chang.** 2004. The cowpox virus host range gene, CP77, affects phosphorylation of eIF2 alpha and vaccinia viral translation in apoptotic HeLa cells. Virology **329:**199–212.
35. **Johnston, J. B., and G. McFadden.** 2004. Technical knockout: understanding poxvirus pathogenesis by selectively deleting viral immunomodulatory genes. Cell Microbiol. **6:**695–705.
36. **Kettle, S., A. Alcami, A. Khanna, R. Ehret, C. Jassoy, and G. L. Smith.** 1997. Vaccinia virus serpin B13R (SPI-2) inhibits interleukin-1beta-converting enzyme and protects virus-infected cells from TNF- and Fas-mediated apoptosis, but does not prevent IL-1beta-induced fever. J. Gen. Virol. **78:**677–685.
37. **Legrand, F. A., P. H. Verardi, L. A. Jones, K. S. Chan, Y. Peng, and T. D. Yilma.** 2004. Induction of potent humoral and cell-mediated immune responses by attenuated vaccinia virus vectors with deleted serpin genes. J. Virol. **78:**2770–2779.
38. **Martin, A. G., and H. O. Fearnhead.** 2002. Apocytochrome c blocks caspase-9 activation and Bax-induced apoptosis. J. Biol. Chem. **277:**50834–50841.
39. **Martinez-Pomares, L., R. J. Stern, and R. W. Moyer.** 1993. The ps/hr gene (B5R open reading frame homolog) of rabbitpox virus controls pock color, is a component of extracellular enveloped virus, and is secreted into the medium. J. Virol. **67:**5450–5462.
40. **Mayr, A., H. Stickl, H. K. Muller, K. Danner, and H. Singer.** 1978. The smallpox vaccination strain MVA: marker, genetic structure, experience gained with the parenteral vaccination and behavior in organisms with a debilitated defence mechanism. Zentbl. Bakteriol. B **167:**375–390. (Author's translation.)
41. **McFadden, G.** 2005. Poxvirus tropism. Nat. Rev. Microbiol. **3:**201–213.
42. **Meiser, A., D. Boulanger, G. Sutter, and J. Krijnse Locker.** 2003. Comparison of virus production in chicken embryo fibroblasts infected with the WR, IHD-J and MVA strains of vaccinia virus: IHD-J is most efficient in trans-Golgi network wrapping and extracellular enveloped virus release. J. Gen. Virol. **84:**1383–1392.
43. **Meyer, H., G. Sutter, and A. Mayr.** 1991. Mapping of deletions in the genome of the highly attenuated vaccinia virus MVA and their influence on virulence. J. Gen. Virol. **72:**1031–1038.
44. **Moss, B.** 1996. Genetically engineered poxviruses for recombinant gene expression, vaccination, and safety. Proc. Natl. Acad. Sci. USA **93:**11341–11348.
45. **Moss, B., and J. L. Shisler.** 2001. Immunology 101 at poxvirus U: immune evasion genes. Semin. Immunol. **13:**59–66.
46. **Ober, B. T., P. Bruhl, M. Schmidt, V. Wieser, W. Gritschenberger, S. Coulibaly, H. Savidis-Dacho, M. Gerencer, and F. G. Falkner.** 2002. Immunogenicity and safety of defective vaccinia virus Lister: comparison with modified vaccinia virus Ankara. J. Virol. **76:**7713–7723.
47. **Ockenhouse, C. F., P. F. Sun, D. E. Lanar, B. T. Wellde, B. T. Hall, K. Kester, J. A. Stoute, A. Magill, U. Krzych, L. Farley, R. A. Wirtz, J. C. Sadoff, D. C. Kaslow, S. Kumar, L. W. Church, J. M. Crutcher, B. Wizel, S. Hoffman, A. Lalvani, A. V. Hill, J. A. Tine, K. P. Guito, C. de Taisne, R. Anders, W. R. Ballou, et al.** 1998. Phase I/IIa safety, immunogenicity, and efficacy trial of NYVAC-Pf7, a pox-vectored, multiantigen, multistage vaccine candidate for Plasmodium falciparum malaria. J. Infect. Dis. **177:**1664–1673.
48. **Oguiura, N., D. Spehner, and R. Drillien.** 1993. Detection of a protein encoded by the vaccinia virus C7L open reading frame and study of its effect on virus multiplication in different cell lines. J. Gen. Virol. **74:**1409–1413.
49. **Paoletti, E.** 1996. Applications of pox virus vectors to vaccination: an update. Proc. Natl. Acad. Sci. USA **93:**11349–11353.
50. **Paoletti, E., J. Tartaglia, and J. Taylor.** 1994. Safe and effective poxvirus vectors—NYVAC and ALVAC. Dev. Biol. Stand. **82:**65–69.
51. **Perkus, M. E., S. J. Goebel, S. W. Davis, G. P. Johnson, K. Limbach, E. K. Norton, and E. Paoletti.** 1990. Vaccinia virus host range genes. Virology **179:**276–286.
52. **Pincus, S., J. Tartaglia, and E. Paoletti.** 1995. Poxvirus-based vectors as vaccine candidates. Biologicals **23:**159–164.
53. **Raengsakulrach, B., A. Nisalak, M. Gettayacamin, V. Thirawuth, G. D. Young, K. S. Myint, L. M. Ferguson, C. H. Hoke, Jr., B. L. Innis, and D. W. Vaughn.** 1999. Safety, immunogenicity, and protective efficacy of NYVAC-JEV and ALVAC-JEV recombinant Japanese encephalitis vaccines in rhesus monkeys. Am. J. Trop. Med. Hyg. **60:**343–349.
54. **Ramsey-Ewing, A., and B. Moss.** 1996. Recombinant protein synthesis in Chinese hamster ovary cells using a vaccinia virus/bacteriophage T7 hybrid expression system. J. Biol. Chem. **271:**16962–16966.
55. **Ramsey-Ewing, A., and B. Moss.** 1995. Restriction of vaccinia virus replication in CHO cells occurs at the stage of viral intermediate protein synthesis. Virology **206:**984–993.
56. **Riedl, S. J., and Y. Shi.** 2004. Molecular mechanisms of caspase regulation during apoptosis. Nat. Rev. Mol. Cell Biol. **5:**897–907.
57. **Risco, C., J. R. Rodriguez, W. Demkowicz, R. Heljasvaara, J. L. Carrascosa, M. Esteban, and D. Rodriguez.** 1999. The vaccinia virus 39-kDa protein forms a stable complex with the p4a/4a major core protein early in morphogenesis. Virology **265:**375–386.
58. **Rivas, C., J. Gil, Z. Melkova, M. Esteban, and M. Diaz-Guerra.** 1998. Vaccinia virus E3L protein is an inhibitor of the interferon (i.f.n.)-induced 2-5A synthetase enzyme. Virology **243:**406–414.
59. **Rodriguez, D., M. Esteban, and J. R. Rodriguez.** 1995. Vaccinia virus A17L gene product is essential for an early step in virion morphogenesis. J. Virol. **69:**4640–4648.
60. **Rodriguez, D., J. R. Rodriguez, J. F. Rodriguez, D. Trauber, and M. Esteban.** 1989. Highly attenuated vaccinia virus mutants for the generation of safe recombinant viruses. Proc. Natl. Acad. Sci. USA **86:**1287–1291.
61. **Rodriguez, J. R., C. Risco, J. L. Carrascosa, M. Esteban, and D. Rodriguez.** 1998. Vaccinia virus 15-kilodalton (A14L) protein is essential for assembly and attachment of viral crescents to virosomes. J. Virol. **72:**1287–1296.
62. **Rowlands, A. G., R. Panniers, and E. C. Henshaw.** 1988. The catalytic mechanism of guanine nucleotide exchange factor action and competitive inhibition by phosphorylated eukaryotic initiation factor 2. J. Biol. Chem. **263:**5526–5533.
63. **Sancho, M. C., S. Schleich, G. Griffiths, and J. Krijnse-Locker.** 2002. The block in assembly of modified vaccinia virus Ankara in HeLa cells reveals new insights into vaccinia virus morphogenesis. J. Virol. **76:**8318–8334.
64. **Sen, G. C.** 2001. Viruses and interferons. Annu. Rev. Microbiol. **55:**255–281.
65. **Shisler, J. L., and B. Moss.** 2001. Immunology 102 at poxvirus U: avoiding apoptosis. Semin. Immunol. **13:**67–72.
66. **Smith, G. L., A. Vanderplasschen, and M. Law.** 2002. The formation and function of extracellular enveloped vaccinia virus. J. Gen. Virol. **83:**2915–2931.
67. **Sutter, G., and B. Moss.** 1992. Nonreplicating vaccinia vector efficiently expresses recombinant genes. Proc. Natl. Acad. Sci. USA **89:**10847–10851.
68. **Sutter, G., and C. Staib.** 2003. Vaccinia vectors as candidate vaccines: the development of modified vaccinia virus Ankara for antigen delivery. Curr. Drug Targets Infect. Disord. **3:**263–271.
69. **Tartaglia, J., W. I. Cox, S. Pincus, and E. Paoletti.** 1994. Safety and immunogenicity of recombinants based on the genetically-engineered vaccinia strain, NYVAC. Dev. Biol. Stand. **82:**125–129.
70. **Tartaglia, J., W. I. Cox, J. Taylor, M. Perkus, M. Riviere, B. Meignier, and E. Paoletti.** 1992. Highly attenuated poxvirus vectors. AIDS Res. Hum. Retrovir. **8:**1445–1447.
71. **Tartaglia, J., M. E. Perkus, J. Taylor, E. K. Norton, J. C. Audonnet, W. I. Cox, S. W. Davis, J. van der Hoeven, B. Meignier, M. Riviere, et al.** 1992. NYVAC: a highly attenuated strain of vaccinia virus. Virology **188:**217–232.
72. **Taylor, J., R. Weinberg, J. Tartaglia, C. Richardson, G. Alkhatib, D. Briedis, M. Appel, E. Norton, and E. Paoletti.** 1992. Nonreplicating viral vectors as potential vaccines: recombinant canarypox virus expressing measles virus fusion (F) and hemagglutinin (HA) glycoproteins. Virology **187:**321–328.
73. **Tsung, K., J. H. Yim, W. Marti, R. M. L. Buller, and J. A. Norton.** 1996. Gene expression and cytopathic effect of vaccinia virus inactivated by psoralen and long-wave UV light. J. Virol. **70:**165–171.
74. **Turner, P., and R. W. Moyer.** 1998. Control of apoptosis by poxviruses. Semin. Virol. **8:**453–469.
75. **Wasilenko, S. T., T. L. Stewart, A. F. Meyers, and M. Barry.** 2003. Vaccinia virus encodes a previously uncharacterized mitochondrial-associated inhibitor of apoptosis. Proc. Natl. Acad. Sci. USA **100:**14345–14350.
76. **Wyatt, L. S., M. W. Carroll, C. P. Czerny, M. Merchlinsky, J. R. Sisler, and B. Moss.** 1998. Marker rescue of the host range restriction defects of modified vaccinia virus Ankara. Virology **251:**334–342.
77. **Yang, Y. L., L. F. Reis, J. Pavlovic, A. Aguzzi, R. Schafer, A. Kumar, B. R. Williams, M. Aguet, and C. Weissmann.** 1995. Deficient signaling in mice devoid of double-stranded RNA-dependent protein kinase. EMBO J. **14:**6095–6106.